Thermodynamics of polymorphism in the AC_{60} (A=K, Rb, Cs) alkali fullerides

L. Gránásy and S. Pekker
Research Institute for Solid State Physics, H-1525 Budapest, P.O.B. 49, Hungary

L. Forró
Departement de Physique, Ecole Polytechnique Federale de Lausanne, 1015-Lausanne, Switzerland
(Received 28 July 1995)

The phase transformations in the AC_{60} (A=K, Rb, Cs) alkali fullerides are studied by differential scanning calorimetry. The relative Gibbs free energies of various phases (fcc, dimer, polymer, etc.) are estimated from the measured transformation temperatures and enthalpies. We find that at low temperatures where the polymer is the stable form, the phase separated ''intermediate state'' of KC_{60} has significantly higher Gibbs free energy.

The alkali fullerides of stoichiometry AC_{60} (A=K, Rb, Cs) have various stable and metastable crystalline modifications. Two stable phases are known: a face-centered-cubic (fcc) rocksalt structure of freely rotating C_{60}^- monomers above ~400 K,[1,2] and an orthorhombic phase[3] containing covalently bonded charged polymer chains below ~400 K.[4–6] By contrast with other AC_{60} salts, the KC_{60} polymer decomposes into an ~100-Å scale mixture of C_{60} and K_3C_{60} at ~370 K.[7] Once formed, this ''intermediate state'' is stable against polymerization below ~450 K.[7] Whether this or the polymer is more stable below ~370 K is unclear. Quenching to different temperatures below 300-K metastable phases appear: (i) a simple cubic (sc) structure of orientationally ordered monomer C_{60}^- ions,[8,9] (ii) an fcc structure with hindered rotation of the C_{60}^- ions (fcc1)[10,11] or (iii) an orthorhombic phase[12,13] consisting $(C_{60}^-)^2$ dimers. Various phase transitions are reported between these phases. In a previous work on RbC_{60}, we mapped the sequence of phase transformations occurring during warming the polymer, dimer, and fcc1 phases.[10] Kosaka *et al.*[8] performed similar studies on RbC_{60} and CsC_{60} and proposed a schematic Gibbs free-energy diagram to explain the phase sequences and stability ranges observed. We calculated the Gibbs free energy of the RbC_{60} phases relative to the high-temperature fcc modification from the relevant thermodynamic data.[11] In this article we estimate the relative Gibbs free energy and the stability range of various (fcc, dimer, polymer, etc.) phases in the AC_{60} (A=K, Rb, Cs) systems on the basis of thermal properties determined by differential scanning calorimetry (DSC).

Polycrystalline powder samples were prepared by solid-state reaction from stoichiometric amounts of alkali metals and high purity (99.9 mol %) C_{60} powder at 650 K. The thermal properties were determined by a Perkin-Elmer DSC-2 calorimeter.

The relative Gibbs free energy of two phases can be calculated from the temperature of the interphase equilibrium T_{eq}, the enthalpy of transformation Q, and the difference of the specific heats ΔC_p as $\Delta G=\Delta H-T\Delta S$, where $\Delta H=Q-\int_T^{T_{eq}}\Delta C_p dT$ and $\Delta S=Q/T_{eq}-\int_T^{T_{eq}}(\Delta C_p/T)dT$. The experimental Q and T_{eq} data used in calculating the relative Gibbs free energies are listed in Table I. The transformation enthalpies were obtained by integrating the thermograms between temperatures chosen suitably below the starting and sufficiently above the end point of the transitions. The equilibrium temperatures were chosen as the onset point of the relevant thermal effects.

The polymer state was produced by long-time (several weeks) heat treatments at ambient temperature for the RbC_{60} and CsC_{60}, and by a 12-h-long heat treatment at 310 K for KC_{60}. On heating above ~340 K, the polymer decomposes into an fcc structure consisting of freely rotating C_{60}^- monomers.[2,10,11] The respective thermograms are shown in Fig. 1. The decomposition of the polymer starts rather slowly (this may reflect the inhomogeneity of the specimens); therefore it is difficult to define a characteristic onset point. We have chosen T_{eq} as the temperature where the massive transformation begins.

The dimer state was prepared by cooling the samples from 500 to 200 K at the highest rate achievable in the calorimeter (~1 K/s). On heating, the dimer was reported to decompose according to the sequence dimer→transient cubic→fcc→polymer→fcc (RbC_{60} and CsC_{60}),[8,10,11] where the transient cubic phase has either an orientationally ordered sc structure[8] or an orientationally disordered fcc structure[10,11] (because of hindered rotation of the C_{60}^- ions). The present thermograms [Figs. 2(a), 3(a), and 4(a)] are consistent with this phase sequence,[14] except that in KC_{60} the polymer decomposes into the intermediate state, which transforms to the high-temperature fcc phase above 445 K. In case of RbC_{60} and CsC_{60} the dimer→transient cubic and transient cubic →fcc transformations overlap; thus the evaluation of the transformation enthalpies is not straightforward. Fortunately, the transient cubic→fcc transformation of RbC_{60} can be studied directly, since the transient cubic phase can be obtained by rapid cooling from 500 to 273 K,[3] and it decomposes following the sequence transient cubic→fcc →polymer→fcc [Fig. 3(a)].[10,11] The peaks of the dimer →transient cubic and transient cubic→fcc transformations in CsC_{60} are of comparable amplitudes and widths [Fig. 4(a)]. It is thus reasonable to assign half of the total heat of the overlapping transitions to each of them. For T_{eq} of the tran-

TABLE I. Thermal properties used in calculating the relative Gibbs free energies. D is for dimer, T for transient cubic phase, P for polymer, and I for intermediate state.

A		$D\rightarrow T$	$T\rightarrow$fcc	$D\rightarrow$fcc	$P\rightarrow$fcc	$P\rightarrow I$	$I\rightarrow$fcc
K	T_{eq} (K)	290	322			380	445
	Q (kJ/mol)	7.7	6.8			14.3	11.2
Rb	T_{eq} (K)		290	280	370		
	Q (kJ/mol)		4.8	10.5	25.8		
Cs	T_{eq} (K)	225	250		360		
	Q (kJ/mol)	4.3	4.3		22.7		

sient cubic→fcc transformation in CsC_{60}, we adopted the onset temperature 250 K recorded by Kosaka *et al.*[8] at a lower heating rate, where the transformations are better separated.

Experimental data of specific heats for the various phases are not available at present. Since the main contribution comes from molecular vibrations of the C_{60}^- ions, which are expected to be essentially unaffected by the crystal structure, it seems reasonable that the specific heats are rather similar if we neglect the differences in the contributions from rotations of the C_{60}^- ions. Therefore, we assume that the specific heat of all phases are the same except for the rotational contribution, which we take as $C_{rot}=(3/2)R$ for the freely rotating fcc, $C_{rot}=R$ for the intermediate phase (1:2 average for the nonrotating K_3C_{60} and the rotating C_{60} regions), and $C_{rot}=0$ for the dimer, polymer, and transient cubic phases. (R is the universal gas constant.) Slight corrections of the calculated Gibbs free energy diagrams may become necessary when accurate experimental data for the specific heats become available.

The calculated Gibbs free energies are shown relative to the freely rotating fcc phase in Figs. 2(b), 3(b), and 4(b). The Gibbs free energy vs temperature diagrams are similar for RbC_{60} and CsC_{60}, where the only stable forms are the polymer (at low temperatures) and the fcc phase of freely rotating C_{60}^- ions (at high temperatures). In KC_{60}, however, the intermediate state has the lowest Gibbs free energy at medium temperatures (~380 to ~445 K), while the fcc is stable above ~445 K, and the polymer is favored below ~380 K. The latter result seems to contradict the finding that after 15 h spent at 350 K no trace of the polymer could be detected in the intermediate state. Note, however, that the intermediate state is composed of finely distributed C_{60} and K_3C_{60} regions.[7] These phases resist polymerization: Pure C_{60} is only able to polymerize under specific conditions, while no polymer of stoichiometry K_3C_{60} exists. Therefore, prior to polymerization the sample has to be homogenized. This means that a high thermodynamic barrier has to be passed, an effect that may efficiently mask the thermodynamic preferences.

The Gibbs free-energy diagram depicts the thermodynamic driving force (ΔG) for various phase transitions. Be-

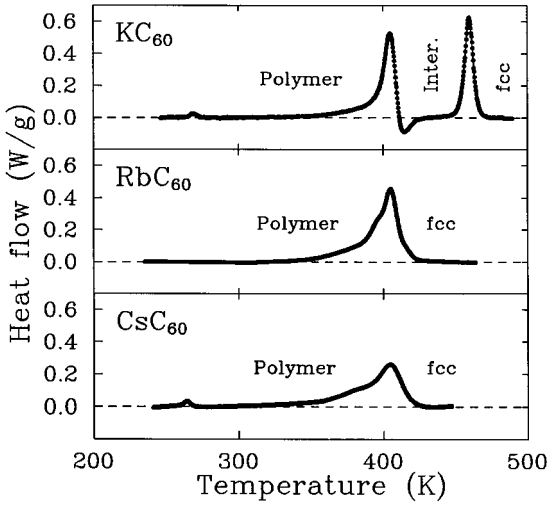

FIG. 1. Decomposition of the AC_{60} (A=K, Rb, Cs) polymers recorded at a heating rate of 20 K/min. (Heat flow is defined so as to be positive for endothermic processes and negative for exothermic tranformations. The small peaks at ~265 K are the rotational transition of pure C_{60}. Their presence indicates a small deviation from stoichiometry.)

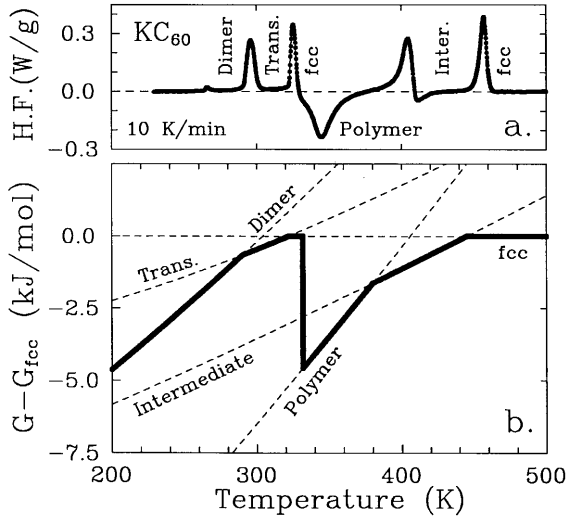

FIG. 2. (a) DSC thermogram recorded on heating the dimer phase of KC_{60} (notation: HF is for heat flow). (b) Gibbs free energy vs temperature curves for various phases relative to the fcc phase stable at high temperatures. The thick solid line shows the phase sequence expected on heating the dimer phase. (Note, that the vertical part is only a schematic representation of the nonequilibrium fcc→polymer transformation and that in heating experiments the transformations start at ~T_{eq}, and the maximum transformation rate occurs at a higher temperature T_{peak}, which depends on the heating rate.)

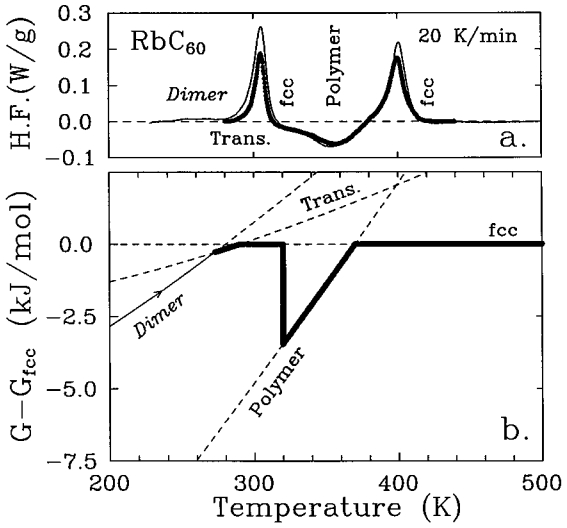

FIG. 3. (a) DSC thermogram recorded on heating the transient cubic (thick solid line) and dimer (thin solid line) phases of RbC_{60}. (b) Gibbs free energy vs temperature curves for various phases relative to the fcc phase stable at high temperatures. [Thick and thin solid lines refer to the decomposition of the transient cubic and dimer phases, respectively. Above the dimer→transient cubic transition (~273 K) the two lines coincide.]

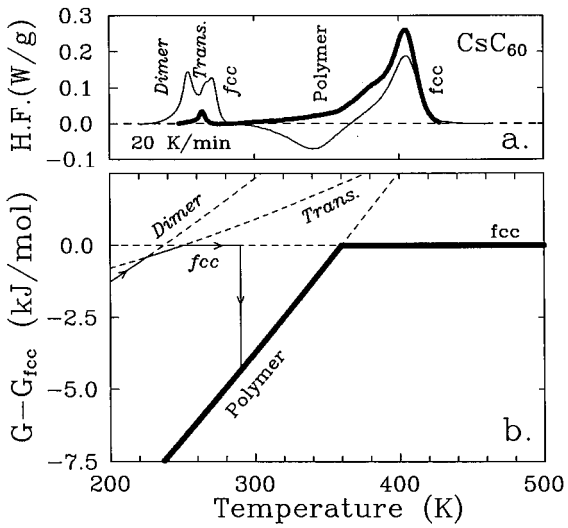

FIG. 4. (a) DSC thermogram recorded on heating the polymer (thick solid line) and dimer (thin solid line) phases of CsC_{60}. (b) Gibbs free energy vs temperature curves for various phases relative to the fcc phase stable at high temperatures. (Thick and thin solid lines refer to the decomposition of the polymer and dimer phases, respectively. Above the fcc→polymer transition the two lines coincide.)

side the driving forces, the transformation mechanism and the time scale of the experiments also influence the phase selection. Since the polymerization takes place with [2+2] cycloaddition for which the C_{60}^{-} ions have to be oriented appropriately, and the dimer phase does not transform directly into the polymer (implying a different interfullerene bonding),[8,10,11,13,15] the rotation of the C_{60}^{-} ions seems to be a precondition of polymerization. Indeed, below the transient cubic→fcc transition ($T_{T-\mathrm{fcc}}$), where the rotation is hindered, the polymerization is slow. The transformations between different polymorphous phases take place without compositional change. In contrast, the formation of the intermediate state is controlled by long-range diffusion; therefore it has to be slower than the other processes. Considering these, one expects that above $T_{T-\mathrm{fcc}}$ the stable phases develop, while at lower temperatures the metastable polymorph of the lowest Gibbs free energy appears.

On the basis of the Gibbs free-energy diagrams and these considerations, the experimental phase sequences can be fully recovered: (i) The decomposition of AC_{60} dimers is expected to follow the phase sequences dimer→transient cubic→fcc→polymer→intermediate→fcc (KC_{60}) or dimer→transient cubic→fcc→polymer→fcc (RbC_{60} and CsC_{60}). The respective Gibbs free-energy routes are shown in Figs. 2(b), 3(b), and 4(b). A remarkable difference is seen in the temperature range of the transient cubic phase (longest for KC_{60}, shortest for RbC_{60}). (ii) On similar grounds, the transient cubic→fcc→polymer→fcc sequence is expected for the decomposition of the transient cubic phase of RbC_{60} [thick line in Fig. 3(b)]. (iii) Finally, decomposition of the polymer into the high-temperature fcc phase is expected to happen either directly [RbC_{60} and CsC_{60}, thick line in Fig. 4(b)] or through the intermediate state (KC_{60}).

In summary, Gibbs free-energy diagrams were calculated from the measured thermal data for the AC_{60} (A=K, Rb, Cs) alkali fullerides, which give the stability range for different phases and explain the phase sequences observed in the experiments. Our results imply that the $x \approx 1$ section of the phase diagrams proposed previously for the K_xC_{60} alkali fullerides[16,17] should be revised by incorporating the polymer as the low-temperature stable phase.

This work was supported by Grant Nos. OTKA-T016057 and OTKA-T4222 of the Hungarian Academy of Sciences, and by Grant Nos. 2100-037318 and 7UNPJ038426 of the Swiss National Foundation for Scientific Research. This research was sponsored by the U.S.-Hungarian Science and Technology Joint Fund under Project No. JFNo 431. The publication fee was provided by the Soros Foundation.

[1] J. Winter and H. Kuzmany, Solid State Commun. **84**, 935 (1992).
[2] Q. Zhu, O. Zhou, J. E. Fischer, A. R. McGhie, W. J. Romanow, R. M. Strongin, M. A. Cichy, and A. B. Smith, Phys. Rev. B **47**, 13 948 (1993).
[3] O. Chauvet, G. Oszlányi, L. Forró, P. W. Stephens, M. Tegze, G. Faigel, and A. Jánossy, Phys. Rev. Lett. **72**, 2721 (1994).
[4] S. Pekker, L. Forró, L. Mihály, and A. Jánossy, Solid State Commun. **90**, 349 (1994).
[5] P. W. Stephens, G. Bortel, G. Faigel, M. Tegze, A. Jánossy, S. Pekker, G. Oszlányi, L. Forró, Nature (London) **370**, 636 (1994).
[6] S. Pekker, A. Jánossy, L. Mihály, O. Chauvet, M. Carrard, and L.

Forró, Science **265**, 1077 (1994).

[7] G. Faigel, G. Bortel, M. Tegze, L. Gránásy, S. Pekker, G. Oszlányi, O. Chauvet, G. Baumgartner, L. Forró, P. W. Stephens, G. Mihály, and A. Jánossy, Phys. Rev. B **52**, 3199 (1995).

[8] M. Kosaka, K. Tanigaki, T. Tanaka, T. Atake, A. Lappas, and K. Prassides, Phys. Rev. B **51**, 12 018 (1995).

[9] A. Lappas, M. Kosaka, K. Tanigaki, and K. Prassides, J. Am. Chem. Soc. **117**, 7560 (1995).

[10] L. Gránásy, T. Kemény, G. Oszlányi, G. Bortel, G. Faigel, M. Tegze, S. Pekker, L. Forró, and A. Jánossy, in *Physics and Chemistry of Fullerenes and Derivatives*, edited by H. Kuzmany, J. Fink, M. Mehring, and S. Roth (World Scientific, Singapore, 1995), p. 331.

[11] L. Gránásy, T. Kemény, G. Oszlányi, G. Bortel, G. Faigel, M. Tegze, S. Pekker, L. Forró, and A. Jánossy (unpublished).

[12] Q. Zhu, D. E. Cox, and J. E. Fischer, Phys. Rev. B **51**, 3966 (1995).

[13] G. Oszlányi, G. Bortel, G. Faigel, M. Tegze, L. Gránásy, S. Pekker, P. W. Stephens, G. Bendele, R. Dinnebier, G. Mihály, A. Jánossy, O. Chauvet, and L. Forró, Phys. Rev. B **51**, 12 228 (1995).

[14] The single dimer→fcc peak of RbC_{60} originates from two overlapping processes (dimer→transient cubic and transient cubic →fcc) that cannot be resolved at the applied heating rate (Ref. 11) but appear separately at a lower heating rate (3 K/min) (Ref. 8).

[15] K. Kamarás, L. Gránásy, D. M. Tanner, and L. Forró, Phys. Rev. B **52**, 11 488 (1995).

[16] D. M. Poirier and J. H. Weaver, Phys. Rev. B **47**, 10 959 (1993).

[17] D. M. Poirier, D. W. Owens, and J. H. Weaver, Phys. Rev. B **51**, 1830 (1995).